

Entangled State Preparation for Non-binary Quantum Computing

Kaitlin N. Smith and Mitchell A. Thornton
Quantum Informatics Research Group
Southern Methodist University, Dallas, Texas, USA
{knsmith, mitch}@smu.edu

Abstract—A common model of quantum computing is the gate model with binary basis states. Here, we consider the gate model of quantum computing with a non-binary radix resulting in more than two basis states to represent a quantum digit, or qudit. Quantum entanglement is an important phenomenon that is a critical component of quantum computation and communications algorithms. The generation and use of entanglement among radix-2 qubits is well-known and used often in quantum computing algorithms. Quantum entanglement exists in higher-radix systems as well although little is written regarding the generation of higher-radix entangled states. We provide background describing the feasibility of multiple-valued logic quantum systems and describe a new systematic method for generating maximally entangled states in quantum systems of dimension greater than two. This method is implemented in a synthesis algorithm that is described. Experimental results are included that demonstrate the transformations needed to create specific forms of maximally entangled quantum states.

I. INTRODUCTION

We are at an exciting age for quantum computation. Noisy intermediate-scale quantum (NISQ) technology is becoming more robust and larger in scale. We are beginning to see experiments, such as those involving molecular structure and linear algebra, that demonstrate the power of quantum machines. While the development of a fault-tolerant quantum computer (QC) is still in progress, promising research causes many people to eagerly anticipate the future of quantum information science (QIS).

Current QIS technology is in an elementary and emerging form. The QC paradigm differs greatly in many aspects from classical computation. When comparing the two models, it is popularly argued that most significant difference is quantum information's ability to demonstrate quantum superposition and entanglement. In particular, quantum entanglement is an important phenomenon that is a critical component of most quantum computational and communications algorithms. The ability to experimentally demonstrate entanglement is significant because this phenomenon enables quantum computing algorithms that exhibit a computational advantage as compared to their classical counterparts. Another very important application of entanglement is that it allows for the implementation of ultra-secure quantum communications protocols. For example, entanglement is necessary for some variations of quantum key distribution (QKD) [1], [2], quantum factoring of composite prime numbers [3], quantum radar [4], quantum teleportation [5], and many other applications.

Most well-known quantum algorithms such as Shor's factoring, Grover's search, and many others depend upon and exploit the properties of entanglement in their implementation. Additionally the entire concept of many QIS systems such as teleportation, quantum communication channels, and others are based on the property of entanglement. The well-known recent Chinese experiments based upon their Micius satellite demonstrated that a quantum channel could be created between the earth and space. The Micius experiments utilized quantum entanglement generators as a key function [6]. The ability to create entangled quantum states for non-binary systems would directly enable these very well-known and accepted results in QIS to be generalized and applied to higher-radix qudit systems.

Most of the emphasis in the literature has been placed on radix $r = 2$ entanglement among qubits. Many of the fundamental characteristics used to represent information are binary in nature, such as particle spin and photon polarization. However, there are also other quantum phenomena that can be used to support information representation with a higher-radix digit set. The advantages of using higher-radix discrete systems for information representation are well-known for conventional information computation and communication systems. In conventional electronics, the use of radices greater than two allow for multiple bits of information to be transmitted and processed per conductor on an integrated circuit, increasing processing bandwidth while simultaneously decreasing on-chip routing congestion due to a decreased number of required conductors. In conventional data communications, it is very common to transmit symbols in modulation schemes such as quadrature-amplitude modulation (QAM) that allow for multiple bits to be communicated per transmitted symbol thus significantly increasing data rates. These and other improvements enjoyed in higher-radix conventional electronic systems can also be advantageous in some QIS systems; however, there is a need for common operations to be specified such as those that generate entanglement.

It is possible to create entangled states in higher-radix systems in a systematic way where qudits initialized to basis states are evolved to a state of entanglement. We present the feasibility of using multiple-valued logic (MVL) quantum systems and provide a novel contribution of a methodology for generating entanglement that we implemented in a synthesis algorithm. The prototype implementation produces entangle-

ment generator circuits that yield maximally-entangled qudits of dimension greater than two. Thus our result can be viewed as a particular form of a quantum state generator. We use operators for creating entanglement in quantum systems of $r > 2$ that were presented in [7], [8]. This work builds on concepts from [7], [8], and the new contribution is a methodology for synthesizing the cascade of gates required to prepare entangled higher-radix states from a fixed starting basis. The techniques described in our work have been prototyped, and the algorithm outputs a description of operators required for entanglement. Experimental results are included that demonstrate the transformations needed to create algorithm-specific quantum states. In previous work, the required structure for entanglement generation was introduced [7]. Although the generalized circuit for a maximally entangled qudit pair was previously described, the choice and placement of $\mathbf{A}_{h,k}$ gates from those available to create a particular entangled state was left undefined. Such a methodology for determining the gates required for entangled state preparation and the accompanying prototype synthesis tool used to generate the quantum algorithm or circuit is a new finding in this paper.

This paper is organized as follows. Important background information that is needed to understand the contribution of this work can be found in Section II. In Section III, the viability of higher-radix quantum computation will be discussed and example realizations of this technology are given. Section IV provides a discussion of the types of operators or gates that we use for higher-radix maximally entangled state preparation. Section V discusses the methodology for developing the generator functions for entangled state preparation and examples and results from our prototype algorithm are included. Finally, Section VI provides a summary and conclusions.

II. QUANTUM INFORMATION PRELIMINARIES

A. Information Representation and Manipulation

The most common unit of quantum information is the radix-2 quantum bit or “qubit.” Qubits represent a linear combination of the basis states $|0_2\rangle = [1 \ 0]^T$ and $|1_2\rangle = [0 \ 1]^T$ where the subscripts are used to refer to the radix value r to avoid confusion when multiple values of r are of discussion. In general, a qubit is represented as

$$|\phi_2\rangle = \alpha |0_2\rangle + \beta |1_2\rangle. \quad (1)$$

Here, α and β are probability amplitudes with complex values, $c \in \mathbb{C}$, that take the form of $c = x + iy$ where i is the imaginary number satisfying $i^2 = -1$. The probability that $|\phi_2\rangle$ is measured as $|0_2\rangle$ is $\alpha^* \alpha = |\alpha|^2$ and the probability that $|\phi_2\rangle$ is measured as $|1_2\rangle$ is $\beta^* \beta = |\beta|^2$ as per the principle known as Born’s rule in quantum mechanics.

Generalizing the qubit construct, higher-radix quantum digits of $r > 2$ are known as “qudits.” A radix- r qudit is a linear combination of r basis states expressed as

$$|\phi_r\rangle = \sum_{i=0}^{r-1} a_i |i_r\rangle. \quad (2)$$

Because the probabilities of occupying any state must sum to unity, the complex-valued coefficients, $a_i \in \mathbb{C}$, satisfy

$$\sum_{i=0}^{r-1} |a_i|^2 = \sum_{i=0}^{r-1} a_i^* a_i = 1. \quad (3)$$

The mathematical model of an overall pure quantum state of a quantum algorithm or circuit is represented as a single vector formed using the individual qubit or qudit states. The vector is of dimension r^n where r is the radix and n is the number of individual qubits or qudits in the system. The quantum state vector, $|\phi_r\rangle$, is thus an element of a finite discrete Hilbert vector space also of dimension r^n denoted as $|\phi_r\rangle \in \mathbb{H}_{r^n}$. The formulation of the overall quantum state vector is accomplished by combining the quantum parallel state of individual qubits or qudits with a tensor or outer product operation. For example, the states $|\phi_r\rangle$ and $|\theta_r\rangle$ would be denoted and combined as $|\phi_r\rangle |\theta_r\rangle = |\phi\theta_r\rangle = |\phi_r\rangle \otimes |\theta_r\rangle$.

A particular algorithm or circuit represents a set of transformation operators that cause the quantum state to evolve in time until the state is eventually collapsed via measurement operations. To preserve Born’s rule before measurement, quantum operations that preserve state must allow for a unity sum of the probability values that derive from the wavefunction’s probability amplitudes. Thus, from a mathematical point of view, the quantum gates that compose an algorithm or circuit can be described as a square unitary transformation matrix, \mathbf{U} , of size $r^n \times r^n$. Quantum state evolution is typically specified in terms of a series or cascade of common operators that are usually in the form of one- or two-qudit operations. The one- or two-qudit operators are expanded to be in the form of unitary $r^n \times r^n$ matrices by forming the tensor product with appropriate identity matrices so that they become transformation operators over the entire quantum state vector. These individual $r^n \times r^n$ transformation matrices are applied in a serial order to the initial quantum state vector resulting in the final evolved state vector. The direct matrix product of the individual serial operations yields the overall transformation matrix for the algorithm or circuit. It should be mentioned that in the gate-model of QIS as used here, the actual implementation can be in the form of application specific hardware, or as the atomic operations in a programmable quantum computer. Thus, our methodology is equally applicable in a QIS circuit synthesis tool or as a technique to be used in a QC compiler. The evolution of a quantum state by a quantum operator is described mathematically as

$$|\phi_r(t_n)\rangle = \mathbf{U} |\phi_r(t_0)\rangle. \quad (4)$$

B. Quantum Superposition

The state of a qubit or qudit is generally specified as a linear combination of a set of r basis functions that span the discrete Hilbert space, \mathbb{H}_{r^n} . Each basis function is scaled by a complex-valued probability amplitude, a_i . A quantum state is said to be in a basis state when all but one of its probability amplitudes are zero-valued. Alternatively, when two or more

probability amplitudes are non-zero, the quantum state is exhibiting the characteristic known as quantum “superposition.” Superposition is convenient since it allows a set of qudits to represent more than one value simultaneously. Superposition is responsible for many of the performance enhancements that quantum algorithms exhibit as compared to conventional algorithms for electronic computers since it essentially provides parallelism of information representation. A single qubit or qudit is said to be “maximally superimposed” when its state vector can be expressed as a linear combination of all basis vectors such that the magnitude of each probability amplitude is equal to $\frac{1}{\sqrt{r^n}}$. Likewise, the overall quantum state of an algorithm or circuit can be maximally superimposed when each constituent qubit or qudit is maximally superimposed. In this case, the maximally superimposed overall state vector is expressed as a sum of scaled basis states where each scalar is $\frac{1}{\sqrt{r^n}}$ and the magnitude squared of the probability amplitude is $\frac{1}{r^n}$. States of partial superposition exist when some qubits or qudits in a quantum algorithm are in a basis state and others are superimposed. Furthermore, if all magnitudes of the probability amplitudes, $|a_i|$, are non-zero but also unequal, then we consider the quantum state to be in superposition, but not maximal superposition. An alternative definition of maximal superposition is in terms of measurement. A quantum state vector is maximally superimposed when a measurement would yield any of the r^n basis states with equal probability.

C. Quantum Entanglement

Entanglement is one of the most unique and significant aspects of QIS because entangled individual quantum elements interact and behave as a single system, even when they are separated by a large distance. Operations and measurements performed on one portion of an entangled group directly influence the state of the other members. With the Hilbert vector space model, it is impossible to describe any single element of an entangled set independently. As an example, the state $|\alpha\beta_2\rangle = a_0|00_2\rangle + a_1|11_2\rangle$ where $|a_i| \neq 0$, represents an entangled state comprised of the two qubits $|\alpha_2\rangle$ and $|\beta_2\rangle$. Mathematically, this state cannot be factored and is therefore inseparable. Measurement of the first qubit, $|\alpha_2\rangle$, gives insight to the value of the second qubit, $|\beta_2\rangle$, without needing a second observation to occur. That is, if the measurement of qubit $|\alpha_2\rangle$ resulted in $|0_2\rangle$, then one would automatically know that the value of $|\beta_2\rangle$ simultaneously collapsed to $|0_2\rangle$ although it was not directly measured. This must be the case because it is impossible for $|\beta_2\rangle$ to be any value other than $|0_2\rangle$ if it is known that $|\alpha_2\rangle = |0_2\rangle$.

When the values of $|a_i|^2$ are equivalent in an entangled state, the state demonstrates maximal entanglement. The example state $|\alpha\beta_2\rangle$ would be maximally entangled if $a_0 = a_1 = \frac{1}{\sqrt{2}}$. Note this is quite different from the definition of maximal superposition since some of the probability amplitude values are zero.

III. HIGHER-RADIX QUANTUM REALIZATIONS

The nature of MVL systems allows for higher density transmission and computation of data because with $r > 2$, more information is stored in each fundamental unit of information [9]. Despite this advantage, classical computing is primarily implemented in binary due to the bistable nature of transistors. For example, MOSFETs can be in saturation or cutoff when they are treated as switching elements. If MVL were to be implemented using MOSFET transistors, it would be necessary to define voltage values in the active region that correspond to specific information values. Thus, an $r = 3$ ternary system would require voltages corresponding to the digits $\{0, 1, 2\}$. From a practical point of view, there would need to be voltage ranges specified, commonly characterized as “noise margins,” that define how much a particular voltage can vary from a specified nominal voltage that represents a logic level. Thus, implementing higher-radix systems in conventional electronics is theoretically possible, but it is rarely done in practice because the advantages of maximizing the number of transistors per unit area that act as binary switches outweighs the advantage gained by using larger transistors that implement switching among r different voltages representing a higher-valued, non-binary radix system. Smaller transistors require smaller rail voltages to operate properly and subdividing these small rail-to-rail voltage intervals into more than two discrete ranges would result in noise margins that are impractical to implement. This is the primary reason that conventional digital electronics has continued to use binary switching models although the advantages of higher-radix information representation are well-known. However, in terms of data communication, it is common to use higher values of radices. As mentioned, QAM is a common example where radices of value 4, 8, 16, 32, and 64 are realized. Generally, these radices are powers of two to allow for simple conversion between transmitted data and the binary processors present in conventional electronic computers.

Today’s quantum devices are noisy and error prone, but this does not mean that higher-radix quantum systems that implement qudits are infeasible. The issues preventing the common use of higher-radix systems for conventional computation, namely the noise margin issue, are not as parasitic in quantum computation. It remains to be seen if other issues will arise that give preference to some computational radices versus others. However, the “noise” present in today’s NISQ QCs has to do with the undesired decoherence of a quantum state rather than issues akin to voltage noise margins, and it is anticipated that these decoherence rates will improve over time. Other QIS research groups have written about the advantages of implementing qudits rather than qubits in QCs that could lead to more powerful quantum computation [10]. The use of higher-radix systems for the representation and processing of information in QIS is potentially viable because of the discrete nature of certain quantum phenomena that is used to carry or represent information. Qudit implementations have been demonstrated experimentally as well as theoretically, and

they have the potential to increase in popularity as quantum technology becomes more mature. Examples of non-binary qudit-based QIP realizations based upon the photon include orbital angular momentum (OAM) [11], time-energy [12], frequency [13], time-phase [14], and location. Qudits implemented with superconducting solid-state technology such as transmon circuits have also been reported [15]. To accommodate to higher-dimensioned quantum systems, especially those that are compatible with radix-2 technology, methodologies for qudit control and readout have been developed [16], [17].

The implementation of higher-radix quantum computation would allow for the compression of data. For example, number of radix- r qudits, M , required to encode the information of N qubits is equal to

$$M = \frac{N}{\log_2(r)}. \quad (5)$$

Increasing the radix of a system greatly increases computation and communication bandwidth. Although including more logic levels provides a certain level of computational advantage, an increase in dimension does increase system complexity because of the added opportunity for introducing error [18]. This presents the question of determining the best radix for quantum computation. This value will be heavily influenced by the number of clearly defined and manipulatable logic levels for a particular technology platform.

To perform meaningful QIP, it is critical to have the ability to prepare higher radix states, such as those where information is entangled, for the execution of quantum algorithms. While there is a considerable amount of past work regarding binary entanglement, there is a limited number of past references regarding the entanglement of qudits. Properties of maximum qudit entanglement have been studied in [19], [20]. Qudit entangled states have also been experimentally demonstrated [21]. However, a general methodology for the synthesis of a state preparation algorithm to yield a maximally entangled state from an arbitrary input state has not been previously reported to the best of our knowledge.

IV. ENTANGLEMENT GENERATORS

A generator function is required for quantum entangled state preparation. For binary or radix-2 quantum information, the Bell state generator is widely known and used to create entangled qubit pairs that are sometimes referred to as ‘‘EPR pairs.’’ A Bell state generator consists of two key components: a single-qubit Hadamard gate that evolves one of the qubit pair into a state of maximal superposition, and a controlled-NOT, C_{NOT} , gate that acts as the entangling gate for the two qubits. The typical use of a Bell state generator is to initialize the qubit pair into one of the four basis states followed by evolving them through the Hadamard and Controlled-NOT gate pair. The Bell state generator can be used as inspiration for a circuit structure that implements higher-radix entangled state preparation. Two key components of such an entanglement generator circuit are thus required to prepare entangled states for any radix. First, one of the involved qudits must be



Fig. 1. Symbol of the radix- r Chrestenson gate, C_r .

transformed into maximal superposition. Second, multi-qubit or qudit interaction is required to combine the states into an mathematically inseparable and therefore entangled form. These transformations can be accomplished with Chrestenson and controlled modulo-add operations, respectively. Entanglement generation with Chrestenson and controlled modulo-add gates is demonstrated for radix-4 quantum systems in [7] and radix-3 quantum systems in [8].

A. The Chrestenson Gate

The Hadamard operator,

$$\mathbf{H} = \frac{1}{\sqrt{2}} \begin{bmatrix} 1 & 1 \\ 1 & -1 \end{bmatrix}. \quad (6)$$

evolves a qubit that is initially in a basis state into a state of maximal superposition. With \mathbf{H} , a basis state qubit is transformed such that it has an equal probability of being measured as either $|0_2\rangle$ or $|1_2\rangle$. For higher-radix systems, the Chrestenson operator is the generalized version of the Hadamard operator and is applied to generate a qudit in maximal superposition. When a qudit in a basis state is applied to a radix- r Chrestenson gate, it is transformed such that it has an equal probability of observation with respect to any of its basis states.

The radix- r Chrestenson transform, C_r , is

$$C_r = \frac{1}{\sqrt{r}} \begin{bmatrix} w_0^0 & w_0^1 & \dots & w_0^{(r-1)} \\ w_1^0 & w_1^1 & \dots & w_1^{(r-1)} \\ \vdots & \vdots & \ddots & \vdots \\ w_{(r-1)}^0 & w_{(r-1)}^1 & \dots & w_{(r-1)}^{(r-1)} \end{bmatrix} \quad (7)$$

where each element in the transformation matrix is a r^{th} root of unity raised to an integral power in the form of $w_k^j = e^{(i\frac{2\pi}{r} \times k) \times j}$ where $j, k = 0, 1, \dots, (r-1)$ [22]. The column index sets the value of j while the row index sets the value for k . The symbol for C_r is pictured in Fig. 1. If the radix-2 Chrestenson transform, C_2 , is derived using Eqn. 7, the Hadamard matrix results, confirming that C_r acts as a generalized superposition operator. More details concerning the theory of Chrestenson transforms can be found in references [22], [23] and an example implementation of a radix-4 Chrestenson gate for location-encoded photonic qudits can be found in references [24], [25].

B. The Controlled Modulo-Add Gate

The NOT operation, also known as the Pauli- X operator,

$$\mathbf{X} = \begin{bmatrix} 0 & 1 \\ 1 & 0 \end{bmatrix}, \quad (8)$$

can be generalized into a modulo- r addition-by- k operator where $r = 2$ and $k = 1$. This is demonstrated by the evolution of qubit $|0_2\rangle$ to be $|((0+1)\bmod 2)_2\rangle = |1_2\rangle$ and $|1_2\rangle$ to be $|((1+1)\bmod 2)_2\rangle = |0_2\rangle$. This alternate viewpoint of the Pauli- \mathbf{X} is useful in the generalization of the Bell state generator into a qudit entanglement generator for radix- r qudits. The controlled version of the Pauli- \mathbf{X} or NOT gate is denoted as the \mathbf{C}_{NOT} gate,

$$\mathbf{C}_{NOT} = \begin{bmatrix} 1 & 0 & 0 & 0 \\ 0 & 1 & 0 & 0 \\ 0 & 0 & 0 & 1 \\ 0 & 0 & 1 & 0 \end{bmatrix}. \quad (9)$$

With respect to modulo- r addition-by- k operators, the \mathbf{C}_{NOT} or controlled- \mathbf{X} gate can be referred to as a controlled-modulo-2 addition-by-1 transformation where the control value is $|1_2\rangle$. This viewpoint is directly applicable to controlled modulo- r addition-by- k operators with activation values from the set $\{0, 1, \dots, (r-1)\}$ for the development of higher-radix maximal entanglement generators.

In the case of radix-2 systems, only two different modulo-2 additions are possible since there are two computational basis vectors, $|0_2\rangle$ and $|1_2\rangle$. Furthermore, one of these is the trivial case of modulo-2 addition-by-zero that results in the identity transformation matrix. Additionally, although most past work in binary QIS consider only the single \mathbf{C}_{NOT} operator wherein the target is activated when the control is $|1_2\rangle$, another variation of a controlled-modulo-add operation could be constructed where the control logic level is $|0_2\rangle$. This variation of the \mathbf{C}_{NOT} operation can also be used in a Bell state generator to prepare entangled qudit states. In general, any value from the set $\{0, 1, \dots, (r-1)\}$ can be used as the activation or control value for a modulo- r addition-by- k gate.

Single qudit modulo-addition operations are represented by $r \times r$ transfer matrices denoted as \mathbf{M}_k for transformations that cause a modulo- k addition with respect to modulus r , as used in [26]. These modulo-addition operators that cause a change of basis are also referred to in the literature as Heisenberg-Weyl operators [27]. The \mathbf{M}_k matrices are all in the form of a permutation matrix and the modulo-0 addition operation is the identity function, or $\mathbf{M}_0 = \mathbf{I}_r$ where \mathbf{I}_r is the $r \times r$ identity matrix. For qudit systems with radix- r , $r > 2$, there are $r-1$ different single non-trivial modulo- r additions. Because the modulo-addition operation can have a controlled form with r available control levels, there exist a total of $r(r-1) = r^2 - r$ non-trivial controlled-modulo-addition operators. The controlled-modulo-addition transformation is denoted as $\mathbf{A}_{h,k}$, where h is the control value that enables the modulo-addition by k operation to occur. $\mathbf{A}_{h,k}$ operates over two qudits of radix r , and its transfer matrix takes the form of the $r^2 \times r^2$ matrix

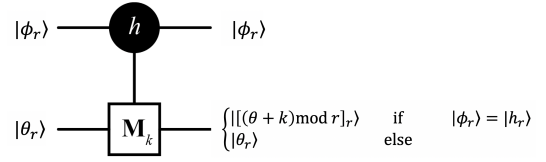


Fig. 2. Symbol of the controlled modulo-add gate, $\mathbf{A}_{h,k}$.

$$\mathbf{A}_{h,k} = \begin{bmatrix} \mathbf{D}_0 & \mathbf{0}_r & \cdots & \cdots & \cdots & \cdots & \mathbf{0}_r \\ \mathbf{0}_r & \mathbf{D}_1 & \mathbf{0}_r & \cdots & \cdots & \cdots & \mathbf{0}_r \\ \vdots & \mathbf{0}_r & \ddots & \mathbf{0}_r & \cdots & \cdots & \mathbf{0}_r \\ \vdots & \vdots & \mathbf{0}_r & \mathbf{D}_j & \mathbf{0}_r & \cdots & \mathbf{0}_r \\ \vdots & \vdots & \vdots & \mathbf{0}_r & \ddots & \mathbf{0}_r & \vdots \\ \vdots & \vdots & \vdots & \vdots & \mathbf{0}_r & \ddots & \mathbf{0}_r \\ \mathbf{0}_r & \mathbf{0}_r & \mathbf{0}_r & \mathbf{0}_r & \cdots & \mathbf{0}_r & \mathbf{D}_{(r-1)} \end{bmatrix}, \quad (10)$$

where, $\mathbf{D}_i = \begin{cases} \mathbf{M}_0 = \mathbf{I}_r, & i \neq h \\ \mathbf{M}_k, & i = h. \end{cases}$

In Eqn. 10, each submatrix along the diagonal is denoted as \mathbf{D}_i and is of dimension $r \times r$. The $\mathbf{A}_{h,k}$ operation only allows the modulo-addition by k transformation to occur on the target whenever the control qudit is in state, $|h_r\rangle$. For a radix-2 system, the $\mathbf{A}_{1,1}$ gate derives the \mathbf{C}_{NOT} transformation of Eqn. 9 when Eqn. 10 is applied. The generalized symbol of $\mathbf{A}_{h,k}$ is pictured in Fig. 2.

C. Demonstration of Higher-Radix Entanglement

A higher-radix maximal entanglement generator for two radix- r qudits takes the form of a Chrestenson gate, \mathbf{C}_r , on the control qudit of $r-1$ different $\mathbf{A}_{h,k}$ gates that operate after the \mathbf{C}_r gate [7]. Each of the control values, h , of the $r-1$ $\mathbf{A}_{h,k}$ gates has a separate and distinct value from the set $\{0, 1, \dots, (r-1)\}$ and each of the modulo-add-by- k target operations, k , of the $r-1$ $\mathbf{A}_{h,k}$ gates, takes on a separate and distinct value from the set $\{1, \dots, (r-1)\}$.

An example radix-3 entanglement generator is pictured in Fig. 3. This circuit includes \mathbf{C}_3 calculated with Eqn. 7 to be

$$\begin{aligned} \mathbf{C}_3 &= \frac{1}{\sqrt{3}} \begin{bmatrix} w_0^0 & w_0^1 & w_0^2 \\ w_1^0 & w_1^1 & w_1^2 \\ w_2^0 & w_2^1 & w_2^2 \end{bmatrix} \\ &= \frac{1}{\sqrt{3}} \begin{bmatrix} 1 & 1 & 1 \\ 1 & e^{\frac{i2\pi}{3} \times 1} & e^{\frac{i2\pi}{3} \times 2} \\ 1 & e^{\frac{i2\pi}{3} \times 2} & e^{\frac{i2\pi}{3} \times 4} \end{bmatrix}. \end{aligned} \quad (11)$$

The $r-1 = 3-1 = 2$ gates in the $\mathbf{A}_{h,k}$ cascade are derived from Eqn. 10 as

$$\mathbf{A}_{1,1} = \begin{bmatrix} 1 & 0 & 0 & 0 & 0 & 0 & 0 & 0 & 0 \\ 0 & 1 & 0 & 0 & 0 & 0 & 0 & 0 & 0 \\ 0 & 0 & 1 & 0 & 0 & 0 & 0 & 0 & 0 \\ \hline 0 & 0 & 0 & 0 & 0 & 1 & 0 & 0 & 0 \\ 0 & 0 & 0 & 1 & 0 & 0 & 0 & 0 & 0 \\ 0 & 0 & 0 & 0 & 1 & 0 & 0 & 0 & 0 \\ \hline 0 & 0 & 0 & 0 & 0 & 0 & 1 & 0 & 0 \\ 0 & 0 & 0 & 0 & 0 & 0 & 0 & 1 & 0 \\ 0 & 0 & 0 & 0 & 0 & 0 & 0 & 0 & 1 \end{bmatrix} \quad (12)$$

and

$$\mathbf{A}_{2,2} = \begin{bmatrix} 1 & 0 & 0 & 0 & 0 & 0 & 0 & 0 & 0 \\ 0 & 1 & 0 & 0 & 0 & 0 & 0 & 0 & 0 \\ 0 & 0 & 1 & 0 & 0 & 0 & 0 & 0 & 0 \\ \hline 0 & 0 & 0 & 1 & 0 & 0 & 0 & 0 & 0 \\ 0 & 0 & 0 & 0 & 1 & 0 & 0 & 0 & 0 \\ 0 & 0 & 0 & 0 & 0 & 1 & 0 & 0 & 0 \\ \hline 0 & 0 & 0 & 0 & 0 & 0 & 0 & 1 & 0 \\ 0 & 0 & 0 & 0 & 0 & 0 & 0 & 0 & 1 \\ 0 & 0 & 0 & 0 & 0 & 0 & 1 & 0 & 0 \end{bmatrix}. \quad (13)$$

In Eqns. 12 and 13, the dashed lines are present to show the placement of the \mathbf{M}_1 in the center sub-matrix and \mathbf{M}_2 in the lower right sub-matrix, respectively. Using the transformation matrices above, the transfer function for the example maximum entanglement generator is

$$\mathbf{T}_{max} = \mathbf{A}_{(2,2)}\mathbf{A}_{(1,1)}(\mathbf{C}_3 \otimes \mathbf{I}_3). \quad (14)$$

To demonstrate the preparation of a fully entangled state with the generator of Fig. 3, the value of the input state $|\phi\theta_3\rangle$ is initialized to the ground state of $|00_3\rangle$. The resulting fully entangled output is

$$\begin{aligned} \mathbf{T}_{max} |00_3\rangle &= \mathbf{A}_{(2,2)}\mathbf{A}_{(1,1)}(\mathbf{C}_3 \otimes \mathbf{I}_3) |00_3\rangle \\ &= \frac{1}{\sqrt{3}} (|00_3\rangle + |11_3\rangle + |22_3\rangle). \end{aligned} \quad (15)$$

In Eqn. 15, the output state is in the form of a maximally entangled state since the basis states present with non-zero probability amplitudes have magnitudes that are equal and are mathematically inseparable by factorization. Therefore, the state is entangled. As another demonstration, an entangled output can be produced with a generator circuit where $h \neq k$ in the controlled modulo-add operations. Consider the transformation matrices of

$$\mathbf{A}_{1,2} = \begin{bmatrix} 1 & 0 & 0 & 0 & 0 & 0 & 0 & 0 & 0 \\ 0 & 1 & 0 & 0 & 0 & 0 & 0 & 0 & 0 \\ 0 & 0 & 1 & 0 & 0 & 0 & 0 & 0 & 0 \\ \hline 0 & 0 & 0 & 0 & 1 & 0 & 0 & 0 & 0 \\ 0 & 0 & 0 & 0 & 0 & 1 & 0 & 0 & 0 \\ 0 & 0 & 0 & 1 & 0 & 0 & 0 & 0 & 0 \\ \hline 0 & 0 & 0 & 0 & 0 & 0 & 1 & 0 & 0 \\ 0 & 0 & 0 & 0 & 0 & 0 & 0 & 1 & 0 \\ 0 & 0 & 0 & 0 & 0 & 0 & 0 & 0 & 1 \end{bmatrix} \quad (16)$$

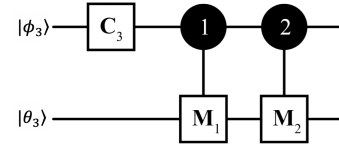


Fig. 3. Example radix-3 maximal entanglement generator.

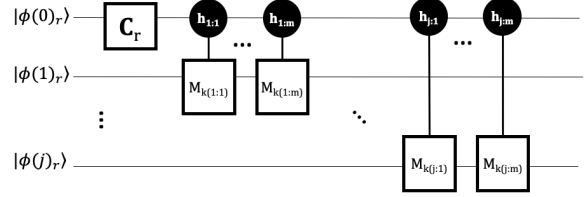


Fig. 4. Generalized structure of circuit needed for radix- r maximal entanglement among n qudits where $j = n - 1$ and $m = r - 1$.

and

$$\mathbf{A}_{2,1} = \begin{bmatrix} 1 & 0 & 0 & 0 & 0 & 0 & 0 & 0 & 0 \\ 0 & 1 & 0 & 0 & 0 & 0 & 0 & 0 & 0 \\ 0 & 0 & 1 & 0 & 0 & 0 & 0 & 0 & 0 \\ \hline 0 & 0 & 0 & 1 & 0 & 0 & 0 & 0 & 0 \\ 0 & 0 & 0 & 0 & 1 & 0 & 0 & 0 & 0 \\ 0 & 0 & 0 & 0 & 0 & 1 & 0 & 0 & 0 \\ \hline 0 & 0 & 0 & 0 & 0 & 0 & 0 & 0 & 1 \\ 0 & 0 & 0 & 0 & 0 & 0 & 1 & 0 & 0 \\ 0 & 0 & 0 & 0 & 0 & 0 & 0 & 1 & 0 \end{bmatrix}. \quad (17)$$

These $\mathbf{A}_{h,k}$ operators can be combined in order to form the maximal entanglement generator

$$\mathbf{T}_{max} = \mathbf{A}_{(2,1)}\mathbf{A}_{(1,2)}(\mathbf{C}_3 \otimes \mathbf{I}_3). \quad (18)$$

If the value of the input state is fixed at $|00_3\rangle$, the transformed state becomes the fully entangled output of

$$\begin{aligned} \mathbf{T}_{max} |00_3\rangle &= \mathbf{A}_{(2,1)}\mathbf{A}_{(1,2)}(\mathbf{C}_3 \otimes \mathbf{I}_3) |00_3\rangle \\ &= \frac{1}{\sqrt{3}} (|00_3\rangle + |12_3\rangle + |21_3\rangle). \end{aligned} \quad (19)$$

Multiple qudits may be transformed into entangled groups if additional cascades of $\mathbf{A}_{h,k}$ operators acting on different targets are added. In these cascades, the rules for h and k values, as defined earlier, are followed. Each group is treated as an independent set where h and k values are appropriate and must not repeat. An illustration of an n qudit maximal entanglement generator structure is included in Fig. 4. In this schematic, each $\mathbf{A}_{h,k}$ operator is characterized by two index values in the form of $j_i : m_i$ where j_i indicates the qudit that acts as the target and m_i is the operator's index within the cascade. The generator of Fig. 4 could be considered a higher-radix generalization of the circuitry needed for the preparation of GHZ states whenever the number of involved qudits, n , is greater than 2.

Data: Radix (r), qudits, input state ($input$), and desired entangled state ($basis$)

Result: Gate sequence, G_i , and associated controls, c_i , and targets, t_i

Set $G \leftarrow []$, $c \leftarrow []$, $t \leftarrow []$;
 $G.append(\text{Chrestenson}(radix))$;
 $c.append(\text{NULL})$;
 $t.append(0)$;

```

for i : 1 ≤ i < qudits do
    for item in basis do
        h ← item[0];
        k ← item[i] + (r - input[i])%r;
        if k ≠ 0 then
            G.append(A(h, k));
            c.append(0);
            t.append(i);
        end
    end
end

```

Algorithm 1: Find entangled state generator circuit

V. NON-BINARY ENTANGLED STATE PREPARATION

It is common knowledge that the Bell state generator can be implemented for radix-2 entangled state preparation. As the dimension of a quantum system grows in size, however, it becomes less intuitive what set of operators are required to prepare a entangled set of basis states where $r > 2$. In addition, it may be necessary to generate a specific entangled state using qudits that are initialized to fixed basis values. For example, many quantum implementations initialize quantum information into a ground state, $|000\dots 00_r\rangle$, that must be used as input to the state preparation generator circuit. For this reason, it is desirable to develop a synthesis technique that derives the gate cascade required to evolve an arbitrary quantum state into a targeted entangled state.

In this work, we outline a methodology for determining the circuit structure needed to create a maximally-entangled, radix- r state with a desired set of basis states from a particular input of qudits. For radix- r , up to r qudits may become maximally entangled so that each qubit index in each linearly-combined basis has a unique value ranging from $[0 : r - 1]$. For this reason, the state preparation circuits generated by this tool can include between two and r qudits. The entangled state generator algorithm has been developed in Python as a prototype synthesis tool that outputs the necessary cascade of Chrestenson and controlled-modulo-add gates to act as the generator for the desired entangled quantum state distribution. The pseudocode that finds the required generator circuit to transform a fixed input basis state into an entangled state is included in Algorithm 1.

Finding the entangled state generator circuit requires the input parameters of radix, number of qudits, input state, and desired entangled basis states. The input basis state is in the form of a list while the desired entangled state is a list of sublists that each represent a basis state in the linear combination. For instance, an input of $|\phi\theta_r\rangle = |00_3\rangle$ is passed as $input = [0, 0]$

and an entangled state of $|\phi\theta_r\rangle = \frac{1}{\sqrt{3}}(|00_3\rangle + |11_3\rangle + |22_3\rangle)$ would be passed as $basis = [[0, 0], [1, 1], [2, 2]]$. It should be noted that the probability amplitude for each of the entangled basis values is set by the column of the C_r matrix with an index equal to the control level in the input qudit state. Therefore, each basis will be multiplied by a radix- r root of unity along with the scale factor of $\frac{1}{\sqrt{r}}$. For example, if the output entangled state in Eqn. 15 is examined where the superimposed control qudit is $|0_3\rangle$, it is clear that each of the basis states has a probability amplitude equal to an element from the 0^{th} index column of the C_3 transform.

Following the structure pictured in Fig. 4, if n total qudits are to be entangled, the first qubit, indexed as $|\phi(0)_r\rangle$ will always be the superimposed qubit that acts as the control for the $A_{h,k}$ gates. Therefore, the C_r operator will act on this qubit before any other operators. Next, $n - 1$ cascades of $A_{h,k}$ gates with appropriate h and k values needed to target each of the remaining qudits must be determined. As a note, to maximally entangle n qudits, $(n - 1)(r - 1)$ total $A_{h,k}$ are required. These gates will always have qudit $|\phi(0)_r\rangle$ as the control qudit and each of the remaining qudits will act as a target for an $A_{h,k}$ cascade in order to become entangled as a group. It is known that each cascade will contain $r - 1$ gates.

Preparing the desired entangled state requires the generation of $n - 1$ $A_{h,k}$ cascades. Each qudit that will act as a target, the qudits ranging from $|\phi(1)_r\rangle$ to $|\phi(j)_r\rangle$, will be iterated through. As seen in the algorithm pseudocode, value of h is derived from the basis in the output state that becomes entangled. The value of k determines the extent of entanglement because it controls what modulo-add- k operation is implemented.

```

r = 3
qudits = 2
basis = [[0,0],[1,1],[2,2]]
input_state = [0,0]

gate_seq = find_ent_gen_ckt(r,qudits,input_state,basis)
for i in gate_seq:
    print("%s : %s"%(i,gate_seq[i]))

Input state: [0, 0]
Desired state: [[0, 0], [1, 1], [2, 2]]

Chrestenson gate: C_3

Needed controlled modulo-additions (Control index 0):
Target qubit index : 1
    A_(1,1)
    A_(2,2)

G : ['C_3', 'A_(1,1)', 'A_(2,2)']
c : [None, 0, 0]
t : [0, 1, 1]

```

Fig. 5. Sample output of generator circuit synthesis to prepare $\frac{1}{\sqrt{3}}(|00_3\rangle + |11_3\rangle + |22_3\rangle)$ from ground state $|00_3\rangle$.

A demonstration of generator circuit synthesis is included in Fig. 5. In this example, the structure of the radix-3 maximal entanglement generator from Fig. 3 is determined using the parameters of the circuit input, $|00_3\rangle$, and the desired entangled quantum state basis values of $|00_3\rangle, |11_3\rangle, |22_3\rangle$.

TABLE I
REQUIRED GENERATOR CIRCUIT COMPONENTS FOR TWO-QUDIT MAXIMALLY ENTANGLED STATE PREPARATION

Input	Basis States of Maximally Entangled Output	C_r Operator	$A_{h,k}$ Operators ($ \phi(0)_r\rangle$ control and $ \phi(1)_r\rangle$ target)
$ 00_2\rangle$ $ 11_2\rangle$	$ 00_2\rangle, 11_2\rangle$	C_2	$A_{1,1}$ $A_{0,1}$
$ 00_3\rangle$ $ 11_3\rangle$ $ 22_3\rangle$	$ 00_3\rangle, 11_3\rangle, 22_3\rangle$	C_3	$A_{1,1}, A_{2,2}$ $A_{0,2}, A_{2,1}$ $A_{0,1}, A_{1,2}$
$ 00_4\rangle$ $ 11_4\rangle$ $ 33_4\rangle$	$ 00_4\rangle, 11_4\rangle, 22_4\rangle, 33_4\rangle$	C_4	$A_{1,1}, A_{2,2}, A_{3,3}$ $A_{0,3}, A_{2,1}, A_{3,2}$ $A_{0,1}, A_{1,2}, A_{2,3}$
$ 00_5\rangle$ $ 22_5\rangle$ $ 44_5\rangle$	$ 00_5\rangle, 11_5\rangle, 22_5\rangle, 33_5\rangle, 44_5\rangle$	C_5	$A_{1,1}, A_{2,2}, A_{3,3}, A_{4,4}$ $A_{0,3}, A_{1,4}, A_{3,1}, A_{4,2}$ $A_{0,1}, A_{1,2}, A_{2,3}, A_{3,4}$
$ 00_6\rangle$ $ 22_6\rangle$ $ 55_6\rangle$	$ 00_6\rangle, 11_6\rangle, 22_6\rangle, 33_6\rangle, 44_6\rangle, 55_6\rangle$	C_6	$A_{1,1}, A_{2,2}, A_{3,3}, A_{4,4}, A_{5,5}$ $A_{0,4}, A_{1,5}, A_{3,1}, A_{4,2}, A_{5,3}$ $A_{0,1}, A_{1,2}, A_{2,3}, A_{3,4}, A_{4,5}$
$ 00_7\rangle$ $ 33_7\rangle$ $ 66_7\rangle$	$ 00_7\rangle, 11_7\rangle, 22_7\rangle, 33_7\rangle, 44_7\rangle, 55_7\rangle, 66_7\rangle$	C_7	$A_{1,1}, A_{2,2}, A_{3,3}, A_{4,4}, A_{5,5}, A_{6,6}$ $A_{0,4}, A_{1,5}, A_{2,6}, A_{4,1}, A_{5,2}, A_{6,3}$ $A_{0,1}, A_{1,2}, A_{2,3}, A_{3,4}, A_{4,5}, A_{5,6}$
$ 00_8\rangle$ $ 33_8\rangle$ $ 77_8\rangle$	$ 00_8\rangle, 11_8\rangle, 22_8\rangle, 33_8\rangle, 44_8\rangle, 55_8\rangle, 66_8\rangle, 77_8\rangle$	C_8	$A_{1,1}, A_{2,2}, A_{3,3}, A_{4,4}, A_{5,5}, A_{6,6}, A_{7,7}$ $A_{0,5}, A_{1,6}, A_{2,7}, A_{4,1}, A_{5,2}, A_{6,3}, A_{7,4}$ $A_{0,1}, A_{1,2}, A_{2,3}, A_{3,4}, A_{4,5}, A_{5,6}, A_{6,7}$
$ 00_9\rangle$ $ 44_9\rangle$ $ 88_9\rangle$	$ 00_9\rangle, 11_9\rangle, 22_9\rangle, 33_9\rangle, 44_9\rangle, 55_9\rangle, 66_9\rangle, 77_9\rangle, 88_9\rangle$	C_9	$A_{1,1}, A_{2,2}, A_{3,3}, A_{4,4}, A_{5,5}, A_{6,6}, A_{7,7}, A_{8,8}$ $A_{0,5}, A_{1,6}, A_{2,7}, A_{3,8}, A_{5,1}, A_{6,2}, A_{7,3}, A_{8,4}$ $A_{0,1}, A_{1,2}, A_{2,3}, A_{3,4}, A_{4,5}, A_{5,6}, A_{6,7}, A_{7,8}$

TABLE II
REQUIRED GENERATOR CIRCUIT COMPONENTS FOR MULTI-QUDIT MAXIMALLY ENTANGLED STATE PREPARATION

Input	Basis States of Maximally Entangled Output	C_r Operator	Target Qudit ($ \phi(0)_r\rangle$ control)	$A_{h,k}$ Operators
$ 012_4\rangle$	$ 000_4\rangle, 111_4\rangle, 222_4\rangle, 333_4\rangle$	C_4	$ \phi(1)_4\rangle$ $ \phi(2)_4\rangle$	$A_{0,3}, A_{2,1}, A_{3,2}$ $A_{0,2}, A_{1,3}, A_{3,1}$
$ 0123_4\rangle$	$ 0000_4\rangle, 1111_4\rangle, 2222_4\rangle, 3333_4\rangle$	C_4	$ \phi(1)_4\rangle$ $ \phi(2)_4\rangle$ $ \phi(3)_4\rangle$	$A_{0,3}, A_{2,1}, A_{3,2}$ $A_{0,2}, A_{1,3}, A_{3,1}$ $A_{0,1}, A_{1,2}, A_{2,3}$
$ 012_5\rangle$	$ 000_5\rangle, 111_5\rangle, 222_5\rangle, 333_5\rangle, 444_5\rangle$	C_5	$ \phi(1)_5\rangle$ $ \phi(2)_5\rangle$	$A_{0,4}, A_{2,1}, A_{3,2}, A_{4,3}$ $A_{0,3}, A_{1,4}, A_{3,1}, A_{4,2}$
$ 0123_5\rangle$	$ 0000_5\rangle, 1111_5\rangle, 2222_5\rangle, 3333_5\rangle, 4444_5\rangle$	C_5	$ \phi(1)_5\rangle$ $ \phi(2)_5\rangle$ $ \phi(3)_5\rangle$	$A_{0,4}, A_{2,1}, A_{3,2}, A_{4,3}$ $A_{0,3}, A_{1,4}, A_{3,1}, A_{4,2}$ $A_{0,2}, A_{1,3}, A_{2,4}, A_{4,1}$
$ 01234_5\rangle$	$ 00000_5\rangle, 11111_5\rangle, 22222_5\rangle, 33333_5\rangle, 44444_5\rangle$	C_5	$ \phi(1)_5\rangle$ $ \phi(2)_5\rangle$ $ \phi(3)_5\rangle$ $ \phi(4)_5\rangle$	$A_{0,4}, A_{2,1}, A_{3,2}, A_{4,3}$ $A_{0,3}, A_{1,4}, A_{3,1}, A_{4,2}$ $A_{0,2}, A_{1,3}, A_{2,4}, A_{4,1}$ $A_{0,1}, A_{1,2}, A_{2,3}, A_{3,4}$

As mentioned previously, all of these basis states will have a probability magnitude of $\frac{1}{\sqrt{3}}$ because that is the value of each of the elements of the 0^{th} column of the C_3 transform.

When generating a maximally-entangled qudit state, it may be necessary to begin with a set of qudits that are initialized to a particular basis before transformation procedures. Depending on the original quantum state, different cascades of $A_{h,k}$ operations must be implemented to achieve a targeted entangled output. To address this scenario, additional examples of synthesized circuit cascades for systems ranging from $r = 2$ to $r = 9$ can be found in Table I for the two-qudit case. This table includes sample input circuit values, found in column one, that target a set of maximally entangled basis states,

found in column two. The required C_r operator is in column three and the synthesized $A_{h,k}$ cascade needed to generate the desired linear combination of basis states is found in column four. Other input qudit and $A_{h,k}$ operator combinations also generate the Table I entangled outputs, but Table I is not all inclusive in the interest of space. As a note, since only two qudits become entangled only $n - 1 = 2 - 1 = 1$ cascade is required. More examples of synthesis are included in Table II. In these results, entangled states including more than two qudits are analyzed for radix-4 and radix-5 systems. These circuit descriptions would be constructed using the form of Fig. 4.

VI. CONCLUSION

We have described how non-binary quantum computation can potentially lead to advantages since more information processing per atomic operation can occur. The technical difficulties that prevented wide-spread adoption of MVL or higher-radix computing with conventional electronic computers is not present in the case of gate-model QCs. Thus, the use of higher-radix computational models should be considered. We also described the fundamental importance of the phenomenon of quantum entanglement and the fact that it is used in virtually all of the well-known QC algorithms and communications protocols that are defined for binary QCs. Next, we described how the bipartite entangled pair generator known as a Bell state generator for binary systems can be used to motivate analogous means of entanglement generation for radix- r algorithms and circuits. The concept of entanglement, and in particular, maximal entanglement, was described for high-radix QIS both mathematically, with several physical examples given. Finally, we derived a systematic methodology for the synthesis of maximal entanglement generation circuits and algorithms and provided an example with our prototype synthesis tool.

In the future, we plan to extend the methodology to account for various forms of partial entanglement such that circuits can be generated that yield subsets of entangled qudits. We also plan to incorporate this methodology into our existing general purpose QC compiler and synthesis tool [28].

REFERENCES

- [1] A. K. Ekert, "Quantum cryptography based on bell's theorem," *Physical review letters*, vol. 67, no. 6, p. 661, 1991.
- [2] D. G. Enzer, P. G. Hadley, R. J. Hughes, C. G. Peterson, and P. G. Kwiat, "Entangled-photon six-state quantum cryptography," *New Journal of Physics*, vol. 4, no. 1, p. 45, 2002.
- [3] P. W. Shor, "Algorithms for quantum computation: Discrete logarithms and factoring," in *Foundations of Computer Science, 1994 Proceedings., 35th Annual Symposium on*. IEEE, 1994, pp. 124–134.
- [4] M. Lanzagorta, "Quantum radar," *Synthesis Lectures on Quantum Computing*, vol. 3, no. 1, pp. 1–139, 2011.
- [5] C. H. Bennett, G. Brassard, C. Crépeau, R. Jozsa, A. Peres, and W. K. Wootters, "Teleporting an unknown quantum state via dual classical and einstein-podolsky-rosen channels," *Physical review letters*, vol. 70, no. 13, p. 1895, 1993.
- [6] J. Yin, Y. Cao, Y.-H. Li, S.-K. Liao, L. Zhang, J.-G. Ren, W.-Q. Cai, W.-Y. Liu, B. Li, H. Dai *et al.*, "Satellite-based entanglement distribution over 1200 kilometers," *Science*, vol. 356, no. 6343, pp. 1140–1144, 2017.
- [7] K. N. Smith and M. A. Thornton, "Entanglement in higher-radix quantum systems," in *IEEE International Symposium on Multiple-Valued Logic (ISMVL)*. IEEE, 2019.
- [8] —, "Higher dimension quantum entanglement generators," *Journal on Emerging Technologies in Computing (to appear)*, 2019.
- [9] D. M. Miller and M. A. Thornton, "Multiple valued logic: Concepts and representations," *Synthesis lectures on digital circuits and systems*, vol. 2, no. 1, pp. 1–127, 2007.
- [10] C. Q. Choi, "Qudits: The real future of quantum computing?" *IEEE Spectrum Magazine*, 2017.
- [11] G. Gibson, J. Courtial, M. J. Padgett, M. Vasnetsov, V. Pas'ko, S. M. Barnett, and S. Franke-Arnold, "Free-space information transfer using light beams carrying orbital angular momentum," *Optics express*, vol. 12, no. 22, pp. 5448–5456, 2004.
- [12] T. Zhong, H. Zhou, R. D. Horansky, C. Lee, V. B. Verma, A. E. Lita, A. Restelli, J. C. Bienfang, R. P. Mirin, T. Gerrits *et al.*, "Photon-efficient quantum key distribution using time–energy entanglement with high-dimensional encoding," *New Journal of Physics*, vol. 17, no. 2, p. 022002, 2015.
- [13] J. M. Lukens and P. Lougovski, "Frequency-encoded photonic qubits for scalable quantum information processing," *Optica*, vol. 4, no. 1, pp. 8–16, 2017.
- [14] N. T. Islam, *High-Rate, High-Dimensional Quantum Key Distribution Systems*. Springer, 2018.
- [15] T. Liu, Q.-P. Su, J.-H. Yang, Y. Zhang, S.-J. Xiong, J.-M. Liu, and C.-P. Yang, "Transferring arbitrary d-dimensional quantum states of a superconducting transmon qudit in circuit qed," *Scientific reports*, vol. 7, no. 1, p. 7039, 2017.
- [16] J. Randall, S. Weidt, E. Standing, K. Lake, S. Webster, D. Murgia, T. Navickas, K. Roth, and W. Hensinger, "Efficient preparation and detection of microwave dressed-state qubits and qutrits with trapped ions," *Physical Review A*, vol. 91, no. 1, p. 012322, 2015.
- [17] J. Randall, A. Lawrence, S. Webster, S. Weidt, N. Vitanov, and W. Hensinger, "Generation of high-fidelity quantum control methods for multilevel systems," *Physical Review A*, vol. 98, no. 4, p. 043414, 2018.
- [18] P. Gokhale, J. M. Baker, C. Duckering, N. C. Brown, K. R. Brown, and F. T. Chong, "Asymptotic improvements to quantum circuits via qutrits," in *ACM/IEEE International Symposium on Computer Architecture (ISCA)*. IEEE, 2019.
- [19] M. Enriquez, I. Wintrowicz, and K. Życzkowski, "Maximally entangled multipartite states: a brief survey," in *Journal of Physics: Conference Series*, vol. 698, no. 1. IOP Publishing, 2016, p. 012003.
- [20] R. Thew, K. Nemoto, A. G. White, and W. J. Munro, "Qudit quantum-state tomography," *Physical Review A*, vol. 66, no. 1, p. 012303, 2002.
- [21] M. Kues, C. Reimer, P. Roztocki, L. R. Cortés, S. Sciara, B. Wetzell, Y. Zhang, A. Cino, S. T. Chu, B. E. Little *et al.*, "On-chip generation of high-dimensional entangled quantum states and their coherent control," *Nature*, vol. 546, no. 7660, p. 622, 2017.
- [22] H. Chrestenson *et al.*, "A class of generalized walsh functions," *Pacific Journal of Mathematics*, vol. 5, no. 1, pp. 17–31, 1955.
- [23] N. Y. Vilenkin, "Concerning a class of complete orthogonal systems," in *Dokl. Akad. Nauk SSSR, Ser. Math*, no. 11, 1947.
- [24] K. N. Smith, T. P. LaFave, D. L. MacFarlane, and M. A. Thornton, "A radix-4 chrestenson gate for optical quantum computation," in *2018 IEEE 48th International Symposium on Multiple-Valued Logic (ISMVL)*. IEEE, 2018.
- [25] K. N. Smith, T. P. LaFave Jr, D. L. MacFarlane, and M. A. Thornton, "Higher-radix chrestenson gates for photonic quantum computation," *Journal of Applied Logics - IfCoLoG Journal of Logics and their Application*, vol. 5, no. 9, pp. 1781–1798, 2018.
- [26] M. A. Thornton, D. W. Matula, L. Spenner, and D. M. Miller, "Quantum logic implementation of unary arithmetic operations," in *Multiple Valued Logic, 2008. ISMVL 2008. 38th International Symposium on*. IEEE, 2008, pp. 202–207.
- [27] R. A. Bertlmann and P. Kramer, "Bloch vectors for qudits," *Journal of Physics A: Mathematical and Theoretical*, vol. 41, no. 23, p. 235303, 2008.
- [28] K. N. Smith and M. A. Thornton, "A quantum computational compiler and design tool for technology-specific targets," in *ACM/IEEE International Symposium on Computer Architecture (ISCA)*. IEEE, 2019.